Seminars in Dialysis

ASDIN

Investigation

Longitudinal Assessment of Hemodynamic Endpoints in Predicting Arteriovenous Fistula Maturation

Ehsan Rajabi-Jagahrgh,* Mahesh K. Krishnamoorthy,* Prabir Roy-Chaudhury,†‡[1] Paul Succop,§ Yang Wang,† Ann Choe,¶ and Rupak K. Banerjee*[1]

*Mechanical Engineering Program, School of Dynamic Systems, University of Cincinnati, Cincinnati, Ohio, †Dialysis Vascular Access Research Group, Department of Internal Medicine, Division of Nephrology and Hypertension, University of Cincinnati, Cincinnati, Ohio, ‡Cincinnati Veterans Administration Medical Center, Cincinnati, Ohio, §Department of Epidemiology and Biostatistics, University of Cincinnati, Cincinnati, Ohio, and ¶Department of Radiology, University of Cincinnati, Cincinnati, Ohio

ABSTRACT

Arteriovenous fistula (AVF) nonmaturation is currently a significant clinical problem; however, the mechanisms responsible for this have remained unanswered. Previous work by our group and others has suggested that anatomical configuration and the corresponding hemodynamic endpoints could have an important role in AVF remodeling. Thus, our *goal* was to assess the longitudinal (temporal) effect of wall shear stress (WSS) on remodeling process of AVFs with two different configurations. The *hypothesis* is that early assessment of hemodynamic endpoints such as temporal gradient of WSS will predict the maturation status of AVF at later time points. Two AVFs with curved (C-AVF) and straight (S-AVF) configurations were created between the femoral artery and vein of each pig. Three pigs were considered in this study and in total six AVFs (three C-AVF and three S-AVF) were created. The CT scan and ultrasound were utilized to numerically evaluate local WSS at 20 cross-sections along the venous segment of AVFs at 2D (D: days), 7D, and 28D postsurgery. These cross-sections were located at 1.5 mm increments from the anastomosis junction. Local WSS values at these cross-sections were correlated with their corresponding luminal area over time. The WSS in C-AVF decreased from 22.3 ± 4.8 dyn/cm^2 at 2D to 4.1 ± 5.1 dyn/cm^2 at 28D, while WSS increased in S-AVF from 13.0 ± 5.0 dyn/cm^2 at 2D to 36.7 ± 5.3 dyn/cm^2 at 28D. Corresponding to these changes in WSS levels, luminal area of C-AVF dilated (0.23 ± 0.14 cm^2 at 2D to 0.87 ± 0.14 cm^2 at 28D) with attendant increase in flow rate. However, S-AVF had minimal changes in area (0.26 ± 0.02 cm^2 at 2D to 0.27 ± 0.03 cm^2 at 28D) despite some increase in flow rate. Our results suggest that the temporal changes of WSS could have significant effects on AVF maturation. Reduction in WSS over time (regardless of initial values) may result in dilation ($p < 0.05$), while increase in WSS may be detrimental to maturation. Thus, creation of AVFs in a specific configuration which results in a decline in WSS over time may reduce AVF maturation failure.

Arteriovenous fistulae (AVFs) are the preferred form of vascular access in patients undergoing hemodialysis. Infection and thrombosis rates in AVFs are lower than polytetrafluroethylene grafts (the other major form of vascular access), with an improvement in patency (1). Despite these advantages, a major problem associated with AVFs is a very high rate of maturation failure (1–5). Recent studies suggest that over 60% of AVFs are unsuitable for dialysis between 4 and 5 months postsurgery and this has been a major impediment to the "Fistula First" initiative (6,7).

Hemodynamics of the AVF is believed to be responsible for its remodeling patterns which may result in either maturation success or failure. However, the exact relationship between the hemodynamic parameters and remodeling patterns is still unclear. Increase in blood flow soon after the creation of AVF is accompanied by increase in wall shear stress (WSS). This induces compensatory changes both in the arterial and venous structure leading to flow-mediated remodeling (8,9). Previous studies have shown that arteries in response to the increased WSS levels dilate to lower the mean WSS over time; thus, restoring baseline WSS (8,10–12). However, the venous response to WSS variation shows variability. Some studies have shown that vein dilates in response to the increased levels of WSS, while others have observed reduction in the luminal area of the vein for similar WSS

Address correspondence to: Rupak K. Banerjee, Professor, Mechanical Engineering Program, School of Dynamic Systems, 593 Rhodes Hall, University of Cincinnati, Cincinnati, OH 45221-0072, e-mail: rupak.banerjee@uc.edu

[1]Rupak Banerjee and Prabir Roy-Chaudhury have contributed equally to this paper.

Seminars in Dialysis—2012
DOI: 10.1111/j.1525-139X.2012.01112.x

levels (13–16). Thus, it is important to explore influence of WSS on remodeling process within the venous segment of an AVF.

In addition, clinical and in vivo studies on the effects of WSS on AVF remodeling have mostly investigated the variation of the average WSS at only one cross-section at different postsurgery time points (8–10,12,17). Thus, effect of variations of local WSS along the arterial and venous segments has been neglected. Moreover, prior numerical studies (18–23) have limited their focus on AVF hemodynamics at only one time point after the creation of AVF. Therefore, these studies are unable to address the dynamic nature of remodeling process over time.

Furthermore, the longitudinal (temporal) effect of early hemodynamic parameters (soon after AVF placement) on the remodeling patterns at later time points is an area that has been generally overlooked in previous studies. Understanding the complex interaction between early hemodynamic parameters (WSS patterns, and flow) and future remodeling patterns could help predicting AVF failure or success in the early stages. Consequently, this will enable clinicians to take proper intervention and thus, improve patient care in end stage renal disease population (24–26). In this regard, the geometry of AVF plays a crucial role as different surgical configurations can result in distinct WSS distributions and thus different remodeling patterns (27).

Here, our hypothesis was that different AVF configurations affect the temporal distribution of WSS which induce distinct remodeling patterns over time. Accordingly, AVFs with two different configurations were created in a pig model to address the following aims: (a) evaluate the effects of two limiting conditions of AVF configurations on hemodynamics (WSS and flow) and its influence on venous remodeling over time; (b) statistically assess the significance of different WSS parameters such as temporal gradient of WSS, early WSS levels, and absolute WSS on the AVF's luminal area over time. From a clinical prospective, goal of this study was to assess whether changes in WSS parameters between sequential time points were associated with clinical endpoints of AVF maturation such as luminal area and flow rates.

Methods

Design of Experiment

The AVFs were created in the curved (C-AVF) and straight (S-AVF) configurations in three pigs between the femoral artery and vein on either limb of 50 kg Yorkshire Cross pigs (Fig. 1A,B). The major difference between two configurations was the higher radius of curvature ($=4.2 \pm 0.3$ mm) in C-AVF whereas it was relatively smaller ($=2.7 \pm 0.1$ mm) in S-AVF (28). The difference between the radii of curvatures of two configurations was statistically significant ($p < 0.05$). Anatomical and flow measurements were performed 2D (D: days), 7D, and 28D after AVF placement. Pigs were sacrificed at either 7D ($n = 1$) or 28D ($n = 2$) postsurgery. One of the pigs was sacrificed at 7D to obtain histological information at an early postsurgery time point. The specific geometry of AVFs at any of the postsurgery time points was reconstructed from the DICOM images obtained through 64 slice CT angiography (Fig. 1C,D). Color Doppler ultrasound (ATL HDI 5000 Ultrasound, ATL, Bothell, WA, USA) was utilized to record the instantaneous velocity pulses at all the postsurgery points from which the average velocity pulses were obtained. Additional details about experimental design, anatomical, and flow measurements are given in our previous studies (27,29).

Computational Fluid Dynamics Analysis

The GAMBIT software (ver. 6.3.2; Ansys Inc, Canonsburg, PA, USA) was used to generate the numerical domain for each of the reconstructed geometries of the AVFs. The AVF flow fields were obtained through computational fluid dynamics (CFD) analyses using the finite volume method. The velocity pulses measured via

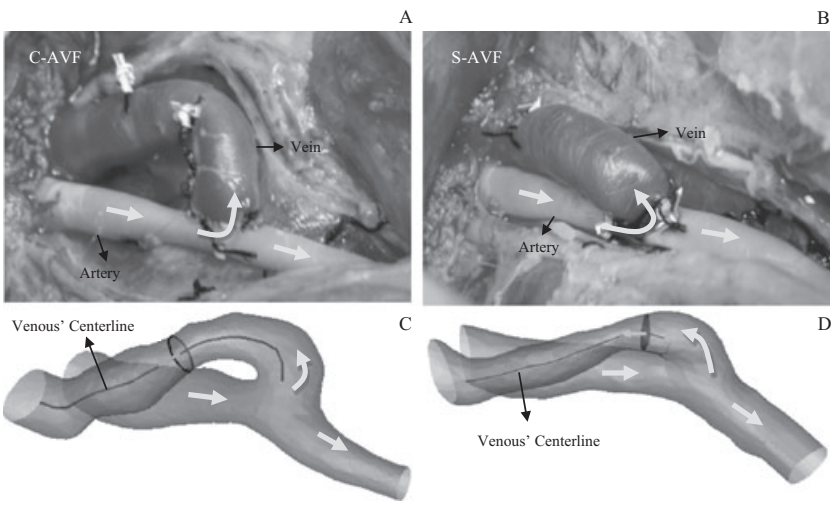

FIG. 1. Surgical configuration of (A) curved (C-AVF) and (B) straight (S-AVF) AVF in a pig model. Femoral artery and vein are specified and white arrows show the flow direction. Reconstructed geometry of (C) C-AVF and (D) S-AVF with a sample cross-section created normal to the venous centerline. The orange vectors correspond to the unit normal vector.

ultrasound at different time points were used as boundary conditions for CFD analysis. Numerical results were validated with the measured flows from the ultrasound (27). Once the flow field of AVF was obtained, 20 cross-sections with 1.5 mm increments from anastomosis junction were created normal to the centerline of vein for all the AVFs at each of the postsurgery time points (Fig. 1C,D). Mean WSS vectors at any boundary node in each cross-section were obtained by averaging WSS over the cardiac cycle. Subsequently, dot product of these vectors and the corresponding unit normal vectors resulted in the mean axial WSS at each of these cross-sections. (Note: Axial WSS is referred to as WSS.) Also, luminal area of the venous segment was measured at these 20 cross-sections. Thus, variation of WSS and luminal area at 20 cross-sections in the venous segment of each AVF was studied over time.

Statistical Analysis

The time-dependent WSS-Area data were regressed using the random effects model. We had 16 repeated measures in time; six for each 28D pigs (three sets at 2D, 7D, and 28D for each C-AVF and S-AVF) and four data points for the 7D pig (two sets at 2D and 7D for each C-AVF and S-AVF). Table 1 shows the matrix of data for this study. It should be noted that each repeated measure involved performing CT scan to obtain anatomical configuration of AVFs and ultrasound to measure flow rates. Subsequently, CFD analysis was performed to evaluate the local WSS and luminal area for 20 cross-sections along the vein of each AVF. Thus, in total, we had 320 (16×20) data points.

The longitudinal measures of WSS (covariate) in the AVFs with two configurations (fixed effects) placed in three pigs (groups) result in a dataset with multilevel structure. The random effects model is an appropriate technique to analyze this type of data (30). Traditional regression techniques, unlike the random effects model, are unable to recognize the multilevel structure of the data which often leads to overestimation or underestimation of the statistical significance of the regression coefficients (30).

Using this method, we can find the correlation between area at 7D or 28D and the various WSS parameters (i.e., temporal gradient of WSS [$\tau' = \frac{dWSS}{dt}$], absolute WSS, and WSS at 2D [WSS_{2D}]) over time. Regression coefficients with p-values less than 0.05 were considered to be statistically significant. The average values of parameters are given in terms of LS-mean values. Here, as our dataset is unbalanced (one pig was sacrificed at 7D), LS-mean is more appropriate to use than arithmetic mean.

Results

Temporal and spatial variations of mean WSS and mean area in the venous segment of the AVFs are described here. Mean luminal area of the vein is considered as a measure of AVF remodeling and an indicator of AVF maturation. Results are presented as mean ± SD.

Effect of WSS on Venous Remodeling

Variations of mean axial WSS and mean area along the venous segment of C-AVF and S-AVF over time are shown in Fig. 2A,B, respectively. Mean WSS and mean area for a specific configuration were obtained by averaging their corresponding values over the 20 cross-sections created along the venous segment. The WSS in the C-AVF decreased from 22.3 ± 4.8 dyn/cm^2 at 2D to 16.9 ± 4.8 dyn/cm^2 at 7D, and to 4.1 ± 5.1 dyn/cm^2 at 28D. However, in S-AVF, WSS increased from 13.0 ± 5.0 dyn/cm^2 at 2D to 20.4 ± 5.0 dyn/cm^2 at 7D, and to 36.7 ± 5.3 dyn/cm^2 at 28D. The decrease in WSS levels of C-AVF was accompanied with an increase in mean area (from 0.23 ± 0.14 cm^2 at 2D to 0.51 ± 0.14 cm^2 at 7D, and to 0.87 ± 0.14 cm^2 at 28D). However, the increase in WSS levels of the S-AVF coincided with almost unchanged luminal area over time

TABLE 1. Data Matrix: Pigs 1 and 2 were sacrificed at 28D postsurgery, while pig 3 was sacrificed 7D after AVF placement. (US stands for ultrasound)

	2D (D: days)			7D			28D		
	CT scan	US	CFD	CT scan	US	CFD	CT scan	US	CFD
Pig 1									
Curved AVF	✔	✔	✔	✔	✔	✔	✔	✔	✔
Number of data points		20			20			20	
Straight AVF	✔	✔	✔	✔	✔	✔	✔	✔	✔
Number of data points		20			20			20	
Pig 2									
Curved AVF	✔	✔	✔	✔	✔	✔	✔	✔	✔
Number of data points		20			20			20	
Straight AVF	✔	✔	✔	✔	✔	✔	✔	✔	✔
Number of data points		20			20			20	
Pig 3									
Curved AVF	✔	✔	✔	✔	✔	✔			
Number of data points		20			20				
Straight AVF	✔	✔	✔	✔	✔	✔			
Number of data points		20			20				

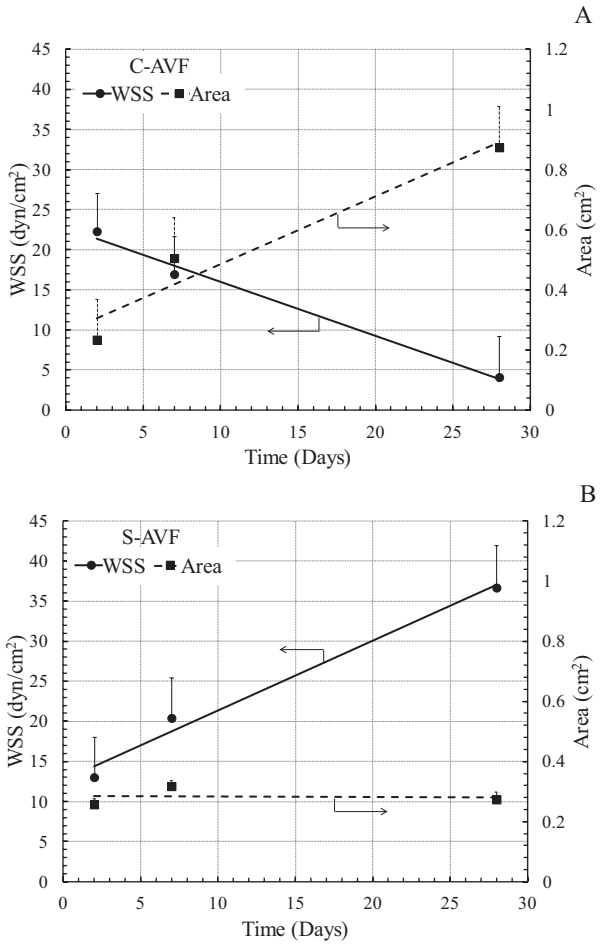

FIG. 2. Variations of mean axial wall shear stress (WSS) and mean area along the venous segment over time for (A) C-AVF and (B) S-AVF.

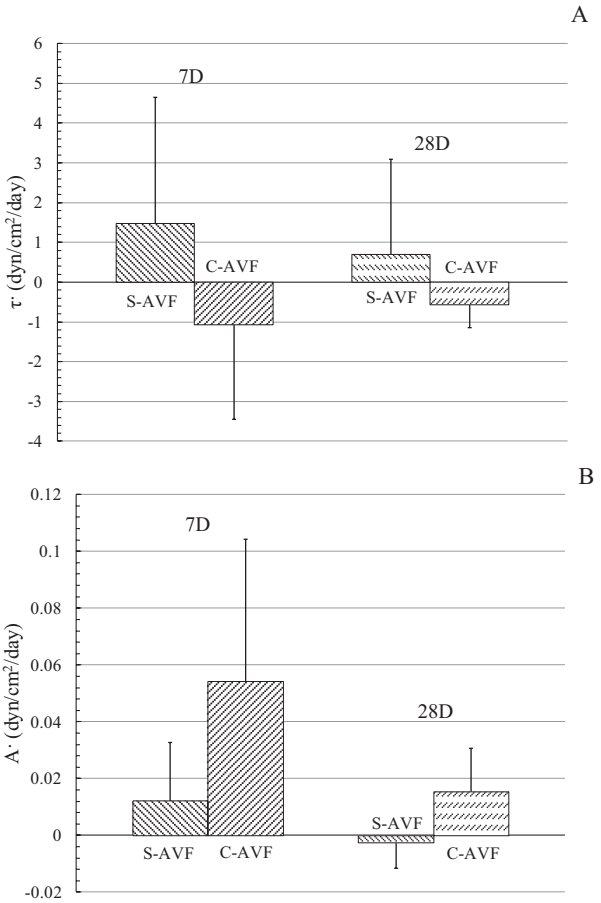

FIG. 3. (A) Temporal gradient of the mean WSS (τ) and (B) temporal gradient of mean area (A) at 7D and 28D for C-AVF and S-AVF.

(from 0.25 ± 0.02 cm^2 at 2D to 0.32 ± 0.02 cm^2 at 7D and to 0.27 ± 0.03 cm^2 at 28D).

Vein Response to the Temporal Gradient of WSS

Temporal gradient of WSS (τ') is defined as the ratio of the difference in later (28D or 7D) WSS from the early (7D or 2D) WSS levels to the corresponding time difference ($\tau' = \frac{WSS_{28D} - WSS_{7D}}{\Delta time}$ and $\tau' = \frac{WSS_{7D} - WSS_{2D}}{\Delta time}$). Also, temporal gradient of luminal area ($A' = \frac{Area_{28D} - Area_{7D}}{\Delta time}$ and $A' = \frac{Area_{7D} - Area_{2D}}{\Delta time}$) is defined the same way as τ'. Here, the differences and trends in WSS at the early time points (2D and 7D) are linked up with later changes (7D and 28D) in luminal area to assess how early WSS trends can influence later luminal area (maturation). Figure 3A,B shows the levels of τ' and A', respectively, at 7D and 28D. τ' at 7D for C-AVF (−1.07 dyn/cm^2/day) is negative as compared to the one for S-AVF (1.48 dyn/cm^2/day), which has also resulted in a larger positive luminal area gradient in the C-AVF (0.05 cm^2/day) vs. S-AVF (0.01 cm^2/day). Furthermore, at 28D, τ' for C-AVF is negative (−0.56 dyn/cm^2/day), which shows reduction in the WSS levels at 28D with respect to the early levels, while S-AVF has a high positive τ' (0.71 dyn/cm^2/day) which reveals the increasing trend of WSS at 28D as compared with 7D. In comparison with these τ' values, A for C-AVF and S-AVF at 28D are 0.015 and −0.0027 cm^2/day, respectively.

Effect of Flow Rate on Venous Remodeling

In addition to luminal area, venous flow rate is one of the important factors to evaluate the AVF maturation. Figure 4 shows the variation of mean venous flow rate for C-AVF and S-AVFs over time. Mean venous flow rates were obtained by averaging the flow rate at venous outlet over the cardiac cycle. Mean flow rate in C-AVF increased from 1125 ± 419 ml/minute at 2D to 2159 ± 419 ml/minute at 7D and to 3700 ± 475 ml/minute at 28D. In comparison with C-AVF, mean flow rates in S-AVF have lower levels at all time points while increasing from 811 ± 343 ml/minute at 2D to 1729 ± 343 ml/minute at 7D and to 1733 ± 406 ml/minute at 28D.

Statistical Model

Here, significance of temporal gradient of WSS (τ'), early WSS (WSS_{2D}), and absolute WSS on luminal area

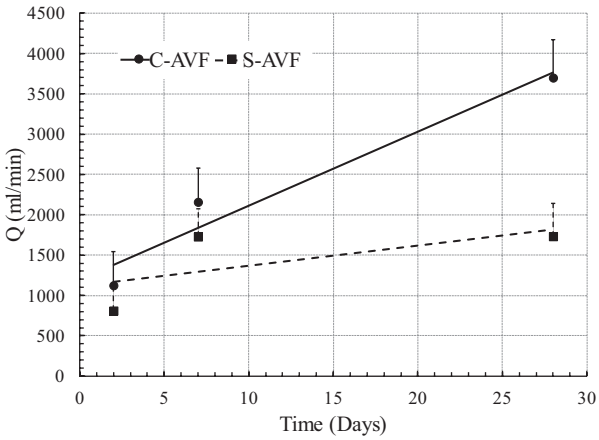

FIG. 4. Variation of mean venous flow rate in C-AVF and S-AVF over time.

of the venous segment is evaluated. Regression model for τ is shown in Table 2. τ' is not significant for S-AVF ($p = 0.776$), while it is significant ($p = 0.01$) for C-AVF with a negative slope ($\beta_1 = -0.021$). Time is significant for both C-AVF and S-AVF with positive ($\beta_2 = 0.343$) and negative ($\beta_2 = -0.073$) slopes, respectively. The regression model for WSS_{2D} is presented in Table 3. The WSS_{2D} is significant for both C-AVF and S-AVF with positive ($\beta_1 = 0.027$) and negative ($\beta_1 = -0.004$) slopes, respectively. Time is also significant with positive ($\beta_2 = 0.564$) and negative ($\beta_2 = -0.082$) slopes for C-AVF and S-AVF, respectively. The interaction between time and WSS_{2D} (time $\times$ WSS_{2D}) is also significant for both C-AVF and S-AVF with negative ($\beta_3 = -0.011$) and positive ($\beta_3 = 0.002$) slopes, respectively. The regression model for the absolute WSS is shown in Table 4. It can be seen that absolute WSS is not a significant factor in predicting the luminal area of AVF in both C-AVF and S-AVF ($p > 0.05$).

Discussion

The ffects of temporal changes of WSS on the luminal area of the AVF with two different configurations were studied for the first time in a pig model. The *major findings* of this research can be summarized as (a) *configuration* of AVF has a strong impact on the WSS distribution and its remodeling patterns; (b) the *temporal gradient of WSS* and not the absolute WSS could be a predictor for clinical maturation; (c) *early WSS* levels soon after AVF placement could also be an important predictor for AVF success or failure.

Effect of Configuration of AVFs on Venous Remodeling

The AVFs were created with curved and straight configurations in a pig model which allowed us to document the local variations of luminal area and WSS along the venous segment of AVFs. The major difference between the surgical configurations of C-AVF and S-AVF was that C-AVFs were created with significantly larger radius of curvature as compared to the S-AVFs (4.21 ± 0.31 mm vs. 2.70 ± 0.08 mm, $p < 0.05$). Although, minimal differences in other geometrical characteristics of AVFs such as anastomosis angle were inevitable, we tried our best to minimize these differences in each group. Therefore, the radius of curvature was kept as the leading difference between the two groups at the day of surgery.

Different geometries of AVF resulted in different WSS values that could trigger distinct remodeling processes over time. The S-AVF induced an increasing trend of WSS over time (from 13.0 ± 5.0 dyn/cm^2 at 2D to 36.7 ± 5.3 dyn/cm^2 at 28D) which accompanied with almost unchanged area (from 0.26 ± 0.02 cm^2 at 2D to 0.27 ± 0.03 cm^2 at 28D). It should be mentioned that increase in WSS levels of S-AVF was associated with simultaneous increase in venous flow rate (perhaps secondary to venous dilation) and almost constant area over time. However, it should be noted that despite the significant increase in flow of S-AVF from 2D (811 ± 343 ml/minute) to 7D (1729 ± 343), the percentage increase in its flow rate from 7D (1729 ± 343 ml/minute) to 28D (1733 ± 406 ml/minute) was only 0.2% ($= 100 \times [(1733 - 1729)/1729]$). During 7D to 28D time points, vasoconstriction in S-AVF resulted in an increase in flow resistance which led to a significant increase in WSS, while the increase in flow rate was minimal. In contrast, C-AVF showed a decreasing trend of WSS over time (from 22.3 ± 4.8 dyn/cm^2 at 2D to 4.1 ± 5.1 dyn/cm^2 at 28D), followed by consistent dilation of area (from 0.23 ± 0.14 cm^2 at baseline to 0.87 ± 0.14 cm^2 at 28D) as well as a very significant increase in flow (from 1125 ± 419 ml/minute at baseline to 3700 ± 475 ml/minute at 28D). This shows that surgical configuration of AVF has a significant impact on the changes in luminal area of the venous segment and ultimately on its maturation or failure.

Effect of Temporal Gradient of WSS on AVF Remodeling

With respect to longitudinal changes of WSS two different remodeling patterns were observed; vasodilation

TABLE 2. Regression Coefficients for the Model: $Area = \beta_0 + \beta_1\tau + \beta_2 time + \varepsilon$

	Straight AVF		Curved AVF	
	Regression coefficient	*p*-value	Regression coefficient	*p*-value
β_0	0.498	0.038	−0.176	0.038
β_1	−0.024	**0.776***	**−0.021**	**0.01**
β_2	**−0.073**	< .0001	**0.343**	< .0001

Bold values are statistically significant, whereas numbers denoted by * do not have statistical significance.

TABLE 3. Regression Coefficients for the Model: $Area = \beta_0 + \beta_1 WSS_{2D} + \beta_2 time + \beta_3 WSS_{2D} \times time + \varepsilon$

	Straight AVF		Curved AVF	
	Regression coefficient	*p*-value	Regression coefficient	*p*-value
β_0	0.481	0.008	−0.166	0.041
β_1	**−0.004**	< 0.0001	**0.027**	< 0.0001
β_2	−0.082	< 0.0001	0.564	< 0.0001
β_3	0.002	< 0.0001	−0.011	< 0.0001

Bold values are statistically significant, whereas numbers denoted by * do not have statistical significance.

TABLE 4. Regression Coefficients for the Model: $Area = \beta_0 + \beta_1 WSS + \beta_2 time + \varepsilon$

	Straight AVF		Curved AVF	
	Regression coefficient	*p*-value	Regression coefficient	*p*-value
β_0	3.912	0.303*	0.150	0.303*
β_1	−0.026	0.801*	−0.009	0.801*
β_2	−1.080	0.790*	0.263	0.877*

Bold values are statistically significant, whereas numbers denoted by * do not have statistical significance.

corresponding to temporal decrease in WSS levels and vasoconstriction associated with longitudinal increase in WSS. In both cases, blood flow has increased over time, albeit with different magnitudes (significant increase in C-AVF and minimal increase in S-AVF); suggesting that flow-mediated remodeling in veins is different than that in arteries. In response to the increased levels of WSS, arteries are known to dilate to normalize the WSS levels (31). However, previous studies (32,33) have shown that venous diameters may shrink in response to the increase in flow rate; similar to the remodeling patterns in S-AVF. In contrast, Corpataux et al. (34) and Langer et al. (13) showed that vein dilates to restore the mean WSS levels over time in both human and animal experiments. This is consistent with the results of C-AVF. These data suggest that the disconnect between the previously described studies could be related to local differences in hemodynamic parameters and profiles. The most plausible cause for localized differences in hemodynamic parameters is of course differences in the anatomical configurations of AVF.

Effect of Early WSS on AVF Remodeling

Acute changes in hemodynamic parameters of the vessels immediately after AVF placement is believed to initiate a remodeling process that can aggressively alter the geometrical and cellular structure of the AVF (11,13,33,35–37). It should be mentioned that despite the availability of several studies on acute flow-mediated remodeling, there are not many studies that explore how vessels adapt in response to early hemodynamics. In our study, C-AVF with higher levels of WSS at 2D (22.3 ± 4.8 dyn/cm^2) has a greater gain in luminal area as compared with S-AVF with early WSS levels of 13.0 ± 5.0 dyn/cm^2 (28D area of C-AVF: 0.87 ± 0.14 cm^2 vs. S-AVF: 0.27 ± 0.03 cm^2). These data suggest that temporal profile of WSS in the early days after the surgery may impose different remodeling patterns in later time points. This is consistent with the findings of Tuttle et al. (37) on the dependency of specific remodeling patterns with the levels of shear stimuli. Authors controlled the WSS levels in mesenteric arteries by regulating blood flow rate. After 2D the luminal diameter remained unchanged in the group with 200% increase in blood flow, while in the 400% group luminal diameter increased. Therefore, different levels of early WSS can trigger distinct remodeling patterns over time. It should be mentioned that this study (37) focused on arterial (not venous) autoregulatory response to flow, and in addition the absolute value of flow was much lower as compared to that present in pig AVFs. Therefore, studying different remodeling patterns in the veins exposed to different levels of early shear stimulus can be of great clinical importance. Our results suggest that veins may experience different remodeling patterns based on the levels of early shear stimulus; however, more studies are needed to explore this phenomenon in detail.

Regression Models of WSS-Dependent Remodeling over Time

Three regression models were considered to find the statistical significance of temporal gradient of WSS (τ'), early WSS, and absolute WSS on luminal area of AVF. It was found that τ' has a negative slope and is significant only in the case of C-AVF. Thus, reduction in WSS levels over time (negative slope) has a positive effect on maturation, while temporal increase (positive slope) in WSS levels is detrimental to maturation. Also, it was found that early WSS levels have a positive slope in C-AVF, while having negative slope in S-AVF. This supports our previous discussion that different early WSS levels may result in distinct remodeling patterns. In addition, absolute value of WSS was found not to correlate with luminal area. Thus, in comparison with absolute WSS, the slope of changes of WSS over time and WSS levels at early stages may be better predictors of future clinical maturation.

It should be mentioned that the sample size was relatively small in this study; however, the repeated measure design of the study allowed statistical inference to be made. Also, WSS and luminal area of 20 cross-sections along the venous segment of each AVF was evaluated over time which compensated for the lesser number of animals for the study. Moreover, it is noteworthy that despite the small sample size, still τ' was found to have a statistically significant effect on variation of luminal area of AVF over time. Thus, this parameter may be a significant parameter to predict the future maturation status of AVF. Therefore, it could be of great clinical importance to conduct similar experiment with larger sample size to explore the influence of initial τ' and early WSS level on future maturation outcome of AVFs.

Conclusion

We showed that configuration of AVF plays a crucial role in remodeling patterns by altering the hemodynamics of AVF. The C-AVF in comparison with S-AVF provides a favorable hemodynamic milieu for remodeling. Our study also introduces early levels of WSS and the temporal variation of WSS as two important hemodynamic parameters that may allow us to predict AVF maturation soon after surgery. In C-AVF, WSS decreases over time which is associated with luminal dilation; however, in S-AVF, WSS increases over time which results in almost unchanged area. Also, early levels of WSS in C-AVF is higher than S-AVF which may reveal that different levels of early WSS can trigger distinct remodeling patterns. Thus, it is of great clinical importance to study the effect of different levels of early shear stimulus and temporal variation of WSS on the remodeling process of the AVFs. It should be noted that both of these parameters can be altered by surgical configuration of AVF. Thus, identifying favorable WSS patterns might help future surgeons to create an optimized AVF configuration that can result in the highest patency.

Accordingly, the clinical significance of this study is twofold:

1. We believe that the combination of early levels of WSS (high or low) together with early initial trends over time (increase or decrease) could be an important predictor of ultimate AVF success or failure. Specifically, as WSS can consider both effects of anatomical configuration and flow rate, it is likely that a combination of the above shear parameters may have a superior predictive power to more conventional, albeit relatively unproven, indicators such as flow and diameter. In particular the early (within 1 week) identification of future AVF dysfunction could allow patients at risk of maturation failure to be placed into aggressive intervention and follow-up protocols to allow for assisted maturation through endovascular or surgical approaches.
2. At a more fundamental level, identification of specific predictive cutoffs for the combination of above hemodynamic parameters (for example, an initial WSS of greater than x plus a percentage decrease in WSS $> y$ in the first week postsurgery) could allow for the computational modeling of an ''ideal'' configuration for an AVF which could then be used by dialysis vascular surgeons.

Finally, we believe that our experimental findings focus on very fundamental interactions between hemodynamics and the vessel wall and so represent a novel approach to the clinical problem of AVF maturation failure. The successful translation of this approach to the clinical arena could play a crucial role in reducing the huge morbidity and economic costs currently associated with AVF maturation failure.

Acknowledgments

This work was funded by a VA Merit Review to Dr. Prabir Roy-Chaudhury.

Conflict of Interest

The authors declare that they have no competing interests.

References

1. Asif A, Roy-Chaudhury P, Beathard GA: Early arteriovenous fistula failure: a logical proposal for when and how to intervene. *Clin J Am Soc Nephrol* 1:332–339, 2006
2. Dixon BS: Why don't fistulas mature? *Kidney Int* 70:1413–1422, 2006
3. Lee T, Chauhan V, Krishnamoorthy M, Wang Y, Arend L, Mistry MJ, El-Khatib M, Banerjee R, Munda R, Roy-Chaudhury P: Severe venous neointimal hyperplasia prior to dialysis access surgery. *Nephrol Dial Transpl* 26:2264–2270, 2011
4. Roy-Chaudhury P, Spergel LM, Besarab A, Asif A, Ravani P: Biology of arteriovenous fistula failure. *J Nephrol* 20:150–163, 2007
5. Kim YO, Choi YJ, Kim JI, Kim YS, Kim BS, Park CW, Song HC, Yoon SA, Chang YS, Bang BK: The impact of intima-media thickness of radial artery on early failure of radiocephalic arteriovenous fistula in hemodialysis patients. *J Korean Med Sci* 21:284–289, 2006
6. III: NKF-K/DOQI Clinical Practice Guidelines for Vascular Access: update 2000. *Am J Kidney Dis* 37:S137–S181, 2001
7. Dixon BS, Novak L, Fangman J: Hemodialysis vascular access survival: upper-arm native arteriovenous fistula. *Am J Kid Dis* 39:92–101, 2002
8. Vita JA, Holbrook M, Palmisano J, Shenouda SM, Chung WB, Hamburg NM, Eskenazi BR, Joseph L, Shapira OM: Flow-induced arterial remodeling relates to endothelial function in the human forearm. *Circulation* 117:3126–3133, 2008
9. Tuka V, Slavikova M, Kasalova Z, Malik J: Factors associated with impaired arterial adaptation to chronically high wall shear rate in the feeding artery of PTFE grafts. *Am J Nephrol* 28:847–852, 2008
10. Girerd X, London G, Boutouyrie P, Mourad JJ, Safar M, Laurent S: Remodeling of the radial artery in response to a chronic increase in shear stress. *Hypertension* 27:799–803, 1996
11. Kamiya A, Togawa T: Adaptive regulation of wall shear stress to flow change in the canine carotid artery. *Am J Physiol* 239:H14–H21, 1980
12. Remuzzi A, Ene-Iordache B, Mosconi L, Bruno S, Anghileri A, Antiga L, Remuzzi G: Radial artery wall shear stress evaluation in patients with arteriovenous fistula for hemodialysis access. *Biorheology* 40:423–430, 2003
13. Langer S, Heiss C, Paulus N, Bektas N, Mommertz G, Rowinska Z, Westenfeld R, Jacobs MJ, Fries M, Koeppel TA: Functional and structural response of arterialized femoral veins in a rodent AV fistula model. *Nephrol Dial Transplant* 24:2201–2206, 2009
14. Berceli SA, Jiang Z, Klingman NV, Schultz GS, Ozaki CK: Early differential MMP-2 and -9 dynamics during flow-induced arterial and vein graft adaptations. *J Surg Res* 134:327–334, 2006

15. Fernandez CM, Goldman DR, Jiang Z, Ozaki CK, Tran-Son-Tay R, Berceli SA: Impact of shear stress on early vein graft remodeling: a biomechanical analysis. *Ann Biomed Eng* 32:1484–1493, 2004
16. Yang B, Shergill U, Fu AA, Knudsen B, Misra S: The mouse arteriovenous fistula model. *J Vasc Interv Radiol* 20:946–950, 2009
17. Ene-Iordache B, Mosconi L, Antiga L, Bruno S, Anghileri A, Remuzzi G, Remuzzi A: Radial artery remodeling in response to shear stress increase within arteriovenous fistula for hemodialysis access. *Endothelium* 10:95–102, 2003
18. Niemann AK, Udesen J, Thrysoe S, Nygaard JV, Fründ ET, Petersen SE, Hasenkam JM: Can sites prone to flow induced vascular complications in a-v fistulas be assessed using computational fluid dynamics? *J Biomech* 43:2002–2009, 2010
19. Carroll GT, McGloughlin TM, Burke PE, Egan M, Wallis F, Walsh MT: Wall shear stresses remain elevated in mature arteriovenous fistulas: a case study. *J Biomech Eng* 133:021003, 2011
20. Ene-Iordache B, Mosconi L, Remuzzi G, Remuzzi A: Computational fluid dynamics of a vascular access case for hemodialysis. *J Biomech Eng* 123:284–292, 2001
21. Migliavacca F, Dubini G: Computational modeling of vascular anastomoses. *Biomech Model Mechanobiol* 3:235–250, 2005
22. Loth F, Fischer PF, Arslan N, Bertram CD, Lee SE, Royston TJ, Shaalan WE, Bassiouny HS: Transitional flow at the venous anastomosis of an arteriovenous graft: potential activation of the ERK1/2 mechanotransduction pathway. *J Biomech Eng* 125:49–61, 2003
23. Carroll G, McGloughlin T, O'Keeffe L, Callanan A, Walsh M: Realistic temporal variations of shear stress modulate MMP-2 and MCP-1 expression in arteriovenous vascular access. *Cell Mol Bioeng* 2:591–605, 2009
24. Lee T, Roy-Chaudhury P, Thakar CV: Improving incident fistula rates: a process of care issue. *Am J Kidney Dis* 57:814–817, 2011
25. Beathard GA: American Society of Diagnostic and Interventional Nephrology Section Editor: Stephen Ash: An interesting case of early arteriovenous fistula failure: how i would code it. *Semin Dial* 17:516–522, 2004
26. Beathard GA, Arnold P, Jackson J, Litchfield T: Aggressive treatment of early fistula failure. *Kidney Int* 64:1487–1494, 2003
27. Krishnamoorthy M, Roy-Chaudhury P, Wang Y, Sinha Roy A, Zhang J, Khoury S, Munda R, Banerjee R: Measurement of hemodynamic and anatomic parameters in a swine arteriovenous fistula model. *J Vasc Access* 9:28–34, 2008
28. Krishnamoorthy M, Banerjee R, Wang Y, Choe A, Rigger D, Roy-Chaudhury P: Influence of anatomic configuration on flow rate and diameter in AV fistula of pig model. *Kidney Int*, 81(8):745–750, 2012
29. Wang Y, Krishnamoorthy M, Banerjee R, Zhang J, Rudich S, Holland C, Arend L, Roy-Chaudhury P: Venous stenosis in a pig arteriovenous fistula model–anatomy, mechanisms and cellular phenotypes. *Nephrol Dial Transpl* 23:525–533, 2008
30. Li B, Lingsma HF, Steyerberg EW, Lesaffre E: Logistic random effects regression models: a comparison of statistical packages for binary and ordinal outcomes. *BMC Med Res Methodol* 11:77, 2011
31. Galt SW, Zwolak RM, Wagner RJ, Gilbertson JJ: Differential response of arteries and vein grafts to blood flow reduction. *J Vasc Surg* 17:563–570, 1993
32. Komai Y, Nakano A, Seki J, Niimi H: Cell morphological changes in venous remodeling induced by arteriovenous grafting in rat limb. *Clin Hemorheol Microcirc* 32:247–259, 2005
33. Misra S, Woodrum DA, Homburger J, Elkouri S, Mandrekar JN, Barocas V, Glockner JF, Rajan DK, Mukhopadhyay D: Assessment of wall shear stress changes in arteries and veins of arteriovenous polytetrafluoroethylene grafts using magnetic resonance imaging. *Cardiovasc Interv Radiol* 29:624–629, 2006
34. Corpataux JM, Haesler E, Silacci P, Ris HB, Hayoz D: Low-pressure environment and remodelling of the forearm vein in Brescia–Cimino haemodialysis access. *Nephrol Dial Transplant* 17:1057–1062, 2002
35. Gusic RJ, Myung R, Petko M, Gaynor JW, Gooch KJ: Shear stress and pressure modulate saphenous vein remodeling ex vivo. *J Biomech* 38:1760–1769, 2005
36. Tran-Son-Tay R, Hwang M, Garbey M, Jiang Z, Ozaki CK, Berceli SA: An experiment-based model of vein graft remodeling induced by shear stress. *Ann Biomed Eng* 36:1083–1091, 2008
37. Tuttle JL, Nachreiner RD, Bhuller AS, Condict KW, Connors BA, Herring BP, Dalsing MC, Unthank JL: Shear level influences resistance artery remodeling: wall dimensions, cell density, and eNOS expression. *Am J Physiol Heart Circ Physiol* 281:H1380–H1389, 2001